

University of Groningen

Photopolymer Resins with Biobased Methacrylates Based on Soybean Oil for Stereolithography

Guit, Jarno; Tavares, Marjory B. L.; Hul, Jerzy; Ye, Chongnan; Loos, Katja; Jager, Jan; Folkersma, Rudy; Voet, Vincent S. D.

Published in:
ACS Applied Polymer Materials

DOI:
[10.1021/acsapm.9b01143](https://doi.org/10.1021/acsapm.9b01143)

IMPORTANT NOTE: You are advised to consult the publisher's version (publisher's PDF) if you wish to cite from it. Please check the document version below.

Document Version
Publisher's PDF, also known as Version of record

Publication date:
2020

[Link to publication in University of Groningen/UMCG research database](#)

Citation for published version (APA):

Guit, J., Tavares, M. B. L., Hul, J., Ye, C., Loos, K., Jager, J., Folkersma, R., & Voet, V. S. D. (2020). Photopolymer Resins with Biobased Methacrylates Based on Soybean Oil for Stereolithography. *ACS Applied Polymer Materials*, 2(2), 949-957. <https://doi.org/10.1021/acsapm.9b01143>

Copyright

Other than for strictly personal use, it is not permitted to download or to forward/distribute the text or part of it without the consent of the author(s) and/or copyright holder(s), unless the work is under an open content license (like Creative Commons).

The publication may also be distributed here under the terms of Article 25fa of the Dutch Copyright Act, indicated by the "Taverne" license. More information can be found on the University of Groningen website: <https://www.rug.nl/library/open-access/self-archiving-pure/taverne-amendment>.

Take-down policy

If you believe that this document breaches copyright please contact us providing details, and we will remove access to the work immediately and investigate your claim.

Downloaded from the University of Groningen/UMCG research database (Pure): <http://www.rug.nl/research/portal>. For technical reasons the number of authors shown on this cover page is limited to 10 maximum.

Photopolymer Resins with Biobased Methacrylates Based on Soybean Oil for Stereolithography

Jarno Guit, Marjory B.L. Tavares, Jerzy Hul, Chongnan Ye, Katja Loos, Jan Jager, Rudy Folkersma, and Vincent S.D. Voet*



Cite This: *ACS Appl. Polym. Mater.* 2020, 2, 949–957



Read Online

ACCESS |



Metrics & More



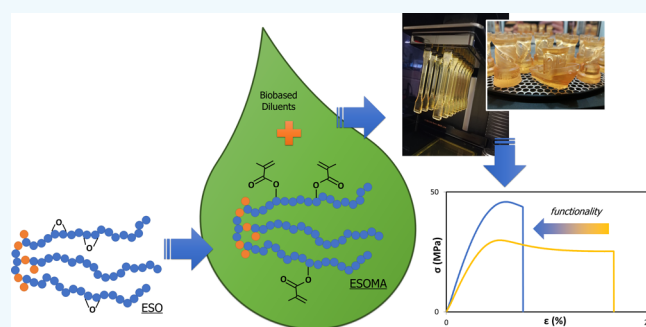
Article Recommendations



Supporting Information

ABSTRACT: The accessibility of renewable materials that are both sustainable and competitive is essential to accommodate the rapid growth in consumption of 3D printing materials. We have developed biobased photopolymer resins based on modified soybean oil for application in commercial stereolithography printers. First, soybean oil methacrylates with various functionalities were successfully synthesized from epoxidized soybean oil as an alternative to commercially available soybean oil acrylate. A library of photoresins was created by mixing up to 80% of the biobased (meth)acrylate oligomers with biobased diluents and a photoinitiator. The resin composition was optimized to achieve a maximum biobased content and a low viscosity. The manufactured parts demonstrated complete layer fusion and accurate print quality. Stiffness and toughness can be tuned by altering the chemical composition or the number of functional groups per oligomer. These biobased materials can be employed to reduce the environmental impact of additive manufacturing while being competitive with current fossil-based resins from commercial manufacturers.

KEYWORDS: biobased, methacrylate, photopolymerization, resin, stereolithography



INTRODUCTION

Additive manufacturing (AM) allows the production of customized parts from a wide range of materials, such as metals, ceramics, thermoplastics polymers, and photopolymer resins. Considering the versatility of AM, it is often promoted as a new industrial revolution.^{1,2} The global market for AM materials is expected to grow by over \$20 billion by the end of 2029,³ of which 22% will be shared by thermosetting photopolymers. Currently, photopolymer resins claim almost half of the market, which is due to their mechanical, chemical, and thermal stability as well as their excellent compatibility with stereolithographic 3D printing.⁴ Commercial resins, however, consist of fossil-based photopolymers that are expensive and limited. Therefore, the availability of renewable alternatives is required to facilitate the increasing demand for AM materials, while reducing their environmental impact.^{5,6}

Lithography-based printing enables layer-by-layer curing of liquid photopolymer resins into products with precisely controlled architectures.⁷ This technology includes both digital light processing (DLP) and laser-based stereolithography (SLA).^{8,9} In comparison to fused filament fabrication (FFF), based on the extrusion of thermoplastic monofilaments, lithography-based printing is superior in terms of accuracy, surface finishing, and resolution.¹⁰ SLA

and DLP are applied in product prototyping and modeling as well as medical device fabrication, such as dental implants^{11,12} and patient-specific scaffolds for tissue regeneration.^{13,14}

Resins for stereolithographic 3D printing require the presence of functional groups to ensure network formation, and the choice of material is therefore limited. Photocurable (meth)acrylate systems undergo radical chain-growth polymerization during 3D printing and consist of an initiator, monomers and oligomers (sometimes referred to as macromonomers).¹⁵ Additives such as stabilizers, fillers or optical absorbers can be added to improve printability or resin properties. The mechanical behavior of thermosetting polymers strongly relates to the molecular architecture of their cross-linked network, which can be influenced by monomer-to-oligomer ratio and number of functional groups.¹⁶ In general, acrylate systems are known for their rapid curing. This results in highly cross-linked and inhomogeneous polymer networks, which tend to be brittle and show low toughness. Methacrylates are less reactive than

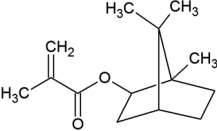
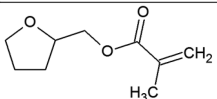
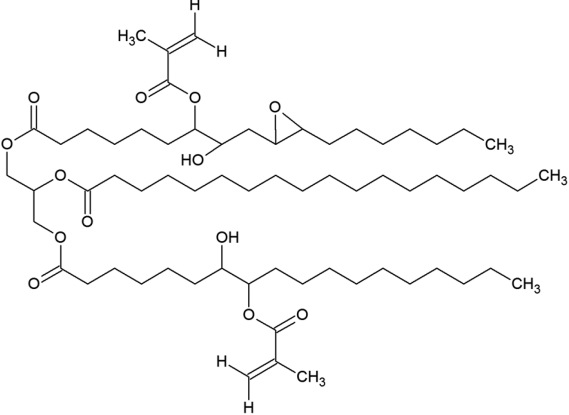
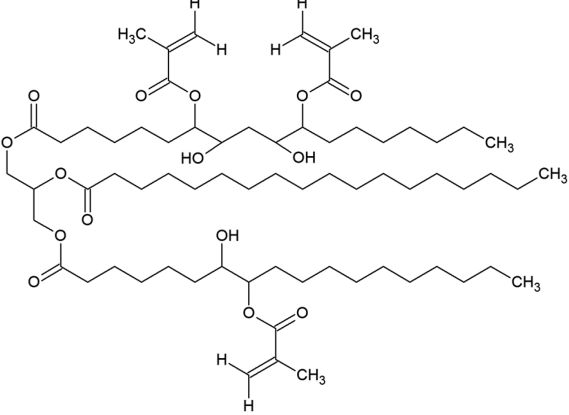
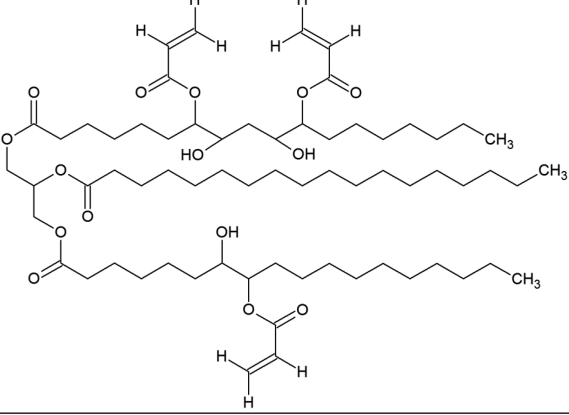
Received: December 2, 2019

Accepted: January 17, 2020

Published: January 21, 2020



Table 1. Characteristics of the Biobased (Meth)acrylate Monomers and Oligomers

Methacrylate	Structural formula	BC %	f	η Pa·s
IBOMA		70.0	1.0	< 0.1
THFMA		55.0	1.0	< 0.1
ESOMA ₂		86.2 ^a	2.3 ^b	10.6 ^c
ESOMA ₃		82.5 ^a	3.0 ^b	21.9 ^c
ESOA ₃		86.4 ^a	3.0	48.8 ^c

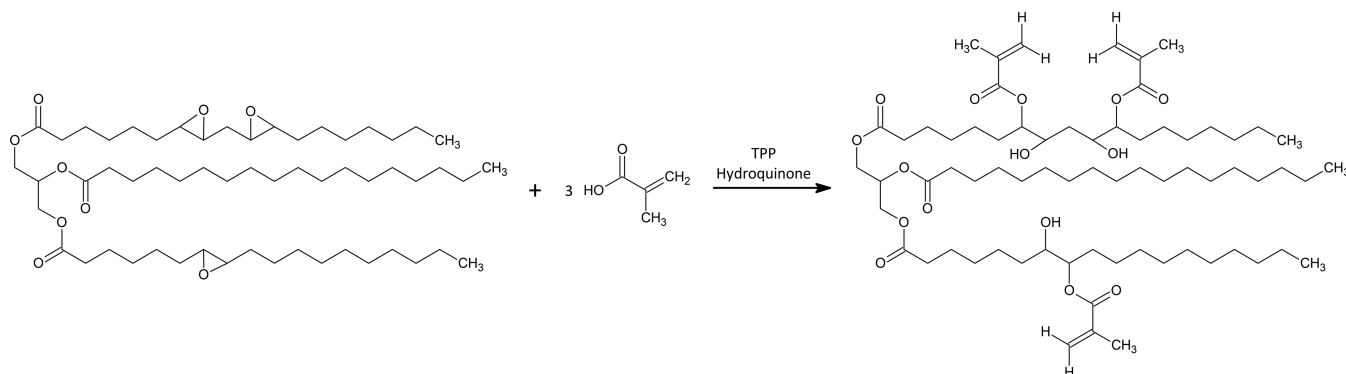
^a Biobased carbon content of methacrylate oligomers (BC_{ESOMA}) is calculated from the ratio between biobased carbon atoms (C_{bio}) and the sum of biobased and fossil-based carbon atoms (C_{total}), according to the following equation: $BC_{ESOMA} = C_{bio}/C_{total} \cdot 100\%$.

^b Methacrylate functionality is calculated from ¹H-NMR data.

^c Viscosity of methacrylate oligomers at shear rate of 50 s⁻¹.

acrylates, and their incorporation into photocurable resins can enhance stiffness and tensile strength.^{17,18}

In recent years, a limited number of academic studies reported the formulation and application of print resins based

Scheme 1. Synthesis of ESOMA₃ via Methacrylation of ESO in the Presence of a Catalyst and Inhibitor

on renewable feedstock such as plants.¹⁹ A photoresin based on D,L-lactide oligomers with methacrylate end-groups was applied in stereolithography, resulting in porous network structures that show potential for tissue engineering applications.^{20,21} Although not specifically reported in this study, (poly)lactide can be produced from biomass such as corn starch and sugar beets.²² Unsaturated polyesters from biobased building blocks, such as succinic, sebacic, and fumaric acid, were used in stereolithography to fabricate 3D bioscaffolds.²³ In another study, renewable lignin-containing resins were generated by mixing commercially available resin components with methacrylated lignin.²⁴ The produced 3D prints exhibited increased ductility, while thermal stability decreased.

Photoresins based on vegetable oils have been developed as well.^{25,26} One example is soybean oil, which is extracted from soybean seeds and is the most produced oil from crops globally.²⁷ Epoxidized soybean oil (ESO) is being manufactured commercially, and methacrylation of ESO leads to soybean oil-based epoxy (meth)acrylates suitable for application in UV-curable coatings with high performance.^{28,29} Epoxidized soybean oil acrylate (ESOA) was already utilized to fabricate shape memory scaffolds using SLA.³⁰ Recently, in our group, a library of photocurable resins was composed using several biobased acrylate monomers and oligomers.^{31,32} The biobased content of the resins ranged from 34 to 67%, and the materials were successfully applied in DLP and SLA 3D printing, leading to well-defined prototypes.

Generally, the mechanical properties of the reported biobased resins are low with respect to commercial standards. Here, we report the development of photocurable resins based on renewable methacrylate oligomers, synthesized from epoxidized soybean oil. Resin formulations are optimized in terms of the monomer-to-oligomer ratio and functionality in order to achieve biobased 3D products with high stiffness and toughness. These bioresins provide a competitive and sustainable alternative to accommodate the rapid growth in consumption of 3D printing materials.

MATERIALS AND METHODS

Materials. Epoxidized soybean oil (ESO, Edenol D81) was supplied by Emery Oleochemicals GmbH. Triphenylphosphine (TPP, 99%), methacrylic acid (99%), and hydroquinone ($\geq 99\%$) were supplied by Merck and used for the modification of ESO. Phenylbis-2,4,6-trimethylbenzoyl phosphine oxide (BAPO, 97%) and trifunctional epoxidized soybean oil acrylate (ESOA₃) were supplied by Merck. Tetrahydrofurfuryl methacrylate (SA6100, THFMA) and

isobornyl methacrylate (SA6105, IBOMA) were supplied by Sartomer. Isopropyl alcohol (IPA) was supplied by Bleko Chemie. Table 1 depicts the characteristics of the biobased (meth)acrylates, i.e. their biobased carbon content (BC), (meth)acrylate functionality (*f*) and viscosity (η). The data was retrieved from the suppliers, unless otherwise noted.

Synthesis of Epoxidized Soybean Oil Methacrylate (ESOMA). Trifunctional epoxidized soybean oil methacrylate (ESOMA₃) was synthesized from ESO in a 1:1 molar ratio (epoxide:methacrylic acid), as depicted in Scheme 1. ESO (200 g, 0.21 mol), methacrylic acid (55.3 g, 0.64 mol), TPP (1% w/w, 2.0 g), and hydroquinone (0.25% w/w, 0.5 g) were added to a 500 mL round bottom flask. The reaction was heated for 46 h at 105 °C while being mechanically stirred at 200 rpm.

For the synthesis of difunctional epoxidized soybean oil methacrylate (ESOMA₂), ESO (200 g, 0.21 mol) and methacrylic acid (36.9 g, 0.43 mol) were added in a molar ratio of 1:0.66 (epoxide:methacrylic acid) to a 500 mL round bottom flask. In addition, TPP (1% w/w, 2.0 g) and hydroquinone (0.25% w/w, 0.5 g) were added to the mixture. The reaction was heated for 46 h at 105 °C, while being mechanically stirred at 200 rpm.

Resin Formulation and Casting. A typical biobased methacrylate photopolymer resin (BMPR) was prepared as follows. A monofunctional diluent (THFMA or IBOMA) and multifunctional oligomer (ESOMA₂, ESOMA₃, or ESOA₃) were added to a cylindrical polypropylene flask, followed by the addition of 1.0% w/w of photoinitiator (BAPO). Next, the mixture was heated for 1 h at 50 °C while being stirred continuously, to ensure homogeneity. Table 2 displays an overview of all resin formulations.

The biobased resins were cast in tensile bar molds by curing both sides of the mold for 5 min in a UV oven ($\lambda = 405$ nm, 39 W). The tensile bars were removed from the mold and postcured for 30 min at 60 °C in the UV oven, identical to the postcuring procedure applied after DLP printing.

Additive Manufacturing. Prior to printing, digital models were processed with CubicreatorLP (Cubicron) software that enables object orientation on the build platform. Subsequently, a Cubicron Lux Full HD DLP 3D printer was employed to build various specimens from BMPR-06, BMPR-09, and BMPR-10 (Table 2). The printer used a halogen lamp ($\lambda = 390$ –450 nm) and a building volume of 100 × 75 × 145 mm³.

Stereolithographic printing was performed at room temperature using preprogrammed settings (named “ABS-Like”) as the default configuration. A layer thickness of 100 μ m was selected. Print settings for exposure time were determined by working curves in triplicate. A microscopic slide was placed on the PDMS cover in the resin tank of the 3D printer. Resin was pipetted on the microscopic slide until it was completely covered. Subsequently, 12 different segments on the microscopic slide were exposed for 1 to 12 s, using an interval of 1 s. Afterward, the unreacted resin was removed by IPA, followed by air-drying. The thickness of the polymerized layers was measured with a digital calliper. Layer thickness (μ m) is shown as a function of exposure time (s) in the working curve (Figure S1).

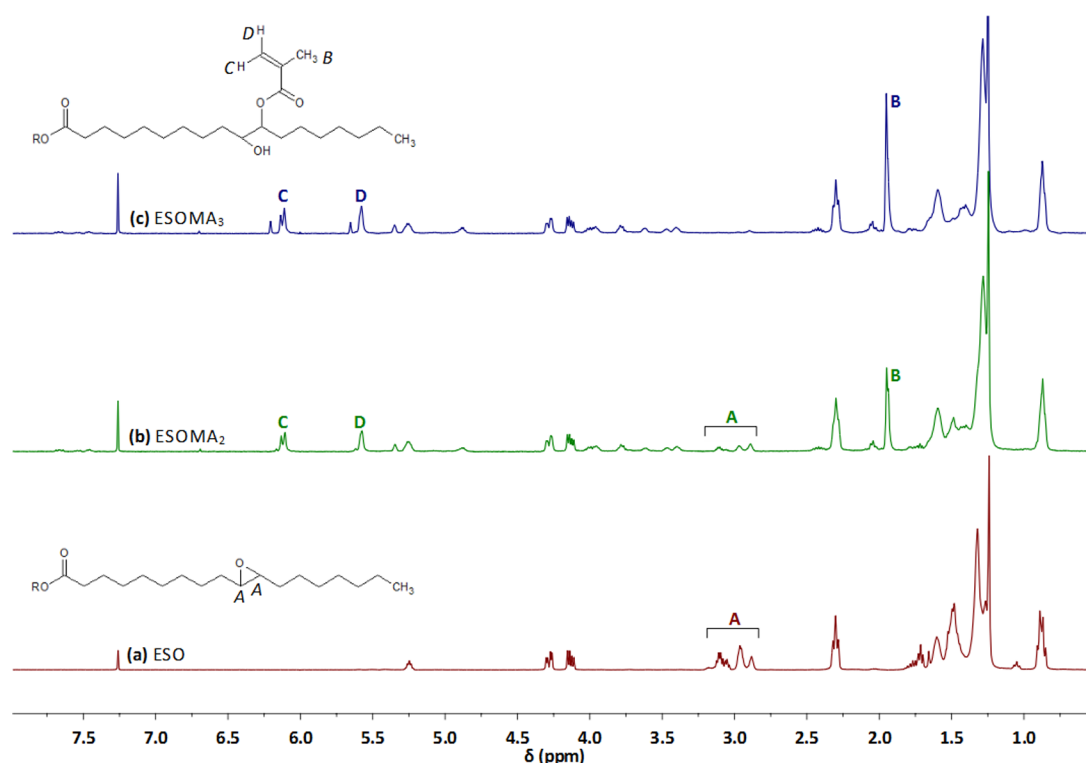


Figure 1. ^1H NMR spectra in CDCl_3 for (a) starting compound ESO (Edenol D81), (b) ESOMA_2 oligomer, and (c) ESOMA_3 oligomer.

The exposure time for the 3D printing process (t_{DLP}) was determined as 105% of the required exposure time for polymerizing a 100 μm layer: $t_{\text{DLP,BMPR06}} = 5.5$ s, $t_{\text{DLP,BMPR09}} = 5.0$ s, and $t_{\text{DLP,BMPR10}} = 5.7$ s. A raft was printed to enhance the attachment to the print platform and was exposed for $6t_{\text{DLP}}$. Next, two layers were exposed for $4t_{\text{DLP}}$, and one layer was exposed for $2t_{\text{DLP}}$; the remaining layers were exposed for t_{DLP} . Tensile bars (ISO 527-2-1 BA), DMA specimens ($60 \times 50 \times 1$ mm 3), and complex shape prototypes with rook tower design³³ were printed normal to the build platform (Figure S2).

After printing, the products were removed from the printing head and soaked for 20 min in an alcohol bath of IPA to remove any unreacted resin, followed by 20 min of air drying. Additionally, the products were postcured in a UV oven ($\lambda = 405$ nm, 39 W) for 30 min at 60 $^\circ\text{C}$.

Characterization. ^1H Nuclear magnetic resonance (^1H NMR) spectra were recorded with a 400 MHz Varian VXR at room temperature. Deuterated chloroform (CDCl_3) was used as the solvent for all samples. Relative peaks were integrated to quantify the functionality of epoxide and methacrylate groups.

An Anton Paar Physica MCR300 parallel-plate rheometer was used to measure the viscosity of the resins according to ISO 6721-10. The geometry of the plates was 50 mm, and the distance between the two geometries was 1 mm. Singular measurements were performed at 20 $^\circ\text{C}$ at a shear rate from 0.1 to 100 s^{-1} .

Fourier transform infrared (FTIR) spectra were recorded in the attenuated total reflection (ATR) mode on a Bruker Vertex 70 spectrometer. In total, 16 scans were performed between 4500 and 400 cm^{-1} with a resolution of 4 cm^{-1} .

Scanning electron microscopy (SEM) was carried out on a FEI Nova NanoSEM 650 operating at an accelerating voltage of 18 kV. The internal helix was sliced out of the rook tower prototype by a razor blade. Prior to imaging, the specimens were coated with 10 nm Au using a Cressington Sputter Coater 208HR.

Dynamic mechanical analysis (DMA) was performed on a RSA II rheometer solids analyzer in tension mode with a strain of 0.1% and at a frequency of 1 Hz to determine the cross-link density (ν_e) of the polymers. Specimens were tested from 40 to 200 $^\circ\text{C}$ with a rate

of 5 $^\circ\text{C}\cdot\text{min}^{-1}$. The storage modulus (G'), loss modulus (G''), and damping factor ($\tan \delta$) were recorded as a function of temperature. The glass transition temperature (T_g) was determined by plotting the $\tan \delta$ as a function of temperature and calculating the peak maximum. The cross-link density was determined from the following equation: $G' = 3\nu_e RT$. T is the absolute temperature 30 K above T_g , G' is the storage modulus in the rubbery plateau region 30 K above T_g . R is the gas constant.

Tensile properties were recorded using an Instron 4301 1kN Series IX tensile tester with a crosshead speed of 5 $\text{mm}\cdot\text{min}^{-1}$ (ISO 527) at room temperature. A minimum of five specimens per sample were analyzed. The elastic modulus (E), strain at break (ϵ_B), stress at peak (σ_M), and deformation energy (U_T) were determined from the stress–strain curves.

RESULTS AND DISCUSSION

Synthesis of Methacrylate Oligomers. ESOMA was synthesized via the methacrylation of epoxidized soybean oil in the presence of TPP as a catalyst and hydroquinone as a cross-linking inhibitor (Scheme 1). ^1H NMR spectra (Figure 1) depict the successful conversion from epoxide to methacrylate moieties.

The reaction of ESO with methacrylic acid in a 1:1 molar ratio results in the full conversion of epoxides, indicated by the disappearance of the signal at 2.8–3.2 ppm corresponding to the epoxide groups (Figure 1a and c). The functionality of ESOMA_3 was calculated from the integral of the methacrylate signals (5.5–6.1 ppm) with respect to the integral representing the CH_3 chain-end (0.8–0.9 ppm),³⁴ giving a methacrylate functionality of 3.0 (Table 1). A detailed structural characterization of ESOMA_3 is presented in Figure S3. Small traces of unreacted methacrylic acid are present (5.6 and 6.2 ppm), since the reaction product was used without further purification. For comparison, ESOMA_3 was also synthesized with excess methacrylic acid, followed by washing with an aqueous KOH solution to remove unreacted

Table 2. Compositions^a and Characteristics of Biobased Resins and Casted Tensile Bars

resins	diluent		oligomer			resin		
	IBOMA (% w/w)	THFMA (% w/w)	ESOMA ₂ (% w/w)	ESOMA ₃ (% w/w)	ESOA ₃ (% w/w)	BC ^b (%)	η^c (Pa·s)	E_{cast} (MPa)
BMPR-01		20			80	80.1	2.78	322
BMPR-02		30			70	77.0	1.05	301
BMPR-03		40			60	73.8	0.84	481
BMPR-04	20				80	83.1	7.20	487
BMPR-05	30				70	81.5	2.87	653
BMPR-06 ^d	40				60	79.8	1.41	809
BMPR-07	20			80		80.0	3.47	692
BMPR-08	30			70		78.8	1.36	876
BMPR-09 ^d	40			60		77.5	0.73	990
BMPR-10 ^d	40		60			79.7	0.52	700

^a1.0% w/w BAPO initiator was added to each resin. ^bBiobased content of resins is calculated from the individual BC of the components, as depicted in Table 1. ^cViscosity of resins at a shear rate of 50 s⁻¹. ^dSelected for stereolithographic 3D printing.

monomers. As a result, no residual methacrylic acid was observed in the spectrum (Figure S4), and the methacrylate functionality is determined to be equal. No significant difference was observed in the elastic modulus of the cured products with or without the small monomer traces, despite their anticipated incorporation in the polymer network. Hence, we decided to proceed with methacrylation in an equimolar ratio, thereby circumventing repetitive washing steps and thus preventing the extensive use of chemicals (KOH, water, or ethyl acetate), which is beneficial for the environment and cost reduction in view of potential commercialization.

ESOMA₂ was prepared by reacting ESO with a limiting amount of methacrylic acid (1:0.66 molar ratio). As expected, the spectrum reveals partially unconverted epoxide moieties (Figure 1b). A methacrylate functionality of 2.3 (Table 1) was calculated from the related integrals.

Resin Formulations. A library of biobased methacrylate photoresins was created by mixing photoinitiator with monofunctional diluents and methacrylate or acrylate oligomers, i.e., ESOMA₂, ESOMA₃, and ESOA₃. Ten formulations with various compositions are depicted in Table 2. The average biobased carbon content of the resins was calculated from the BC of the individual components (Table 1) and ranges from 74 to 83%.

The printability of a resin is largely affected by its viscosity. In general, a viscosity below 2 Pa·s is desired to allow appropriate recoating of the resin during stereolithographic 3D printing.^{35,36} For instance, commercial manufactures, such as Autodesk and Formlabs, use viscosities of 0.44 and 1.6 Pa·s for their fossil-based standard clear resins.³¹ Table 2 displays the bioresin viscosities at a high shear rate of 50 s⁻¹, typical for the printing process.³⁷ As anticipated, the viscosity decreases with an increasing amount of diluent, which is revealed in the series: BMPR-01 → BMPR-03, BMPR-04 → BMPR-06, and BMPR-07 → BMPR-09 (Figure S5). The incorporation of acrylate oligomer leads to a higher resin viscosity compared to the use of methacrylate oligomers due to the addition of more viscous ESOA₃ with respect to ESOMA₂ and ESOMA₃ (Table 1).

All formulated photoresins were cured in tensile bar molds and subsequently subjected to a stress–strain analysis to determine the E modulus (E_{cast}). Increasing the relative amount of monofunctional diluent results in products with a significantly higher modulus (Table 2), related to the more dense polymer network that is formed while curing. The

formulations including IBOMA instead of THFMA give rise to a higher stiffness as well, due to the more rigid structure of IBOMA.

BMPR-06, BMPR-09, and BMPR-10 were selected for application in stereolithographic 3D printing. BMPR-06 and BMPR-09, based on ESOA₃ and ESOMA₃ oligomers, respectively, show a low viscosity (<2.0 Pa·s) in combination with the promise of a high E modulus. ESOMA₂-containing BMPR-10 is taken into account to determine the effect of methacrylate functionality on the mechanical performance.

Stereolithographic 3D Printing. The required exposure time for the print job was determined from the working curves of the selected bioresins (Figure S1), as described in the Materials and Methods section. BMPR-06, BMPR-09, and BMPR-10 were successfully applied in the DLP 3D printing process. The network formation of biobased methacrylate resins was confirmed by FTIR analysis of BMPR-10 (Figure 2). Double bonds in IBOMA and ESOMA₂ are converted

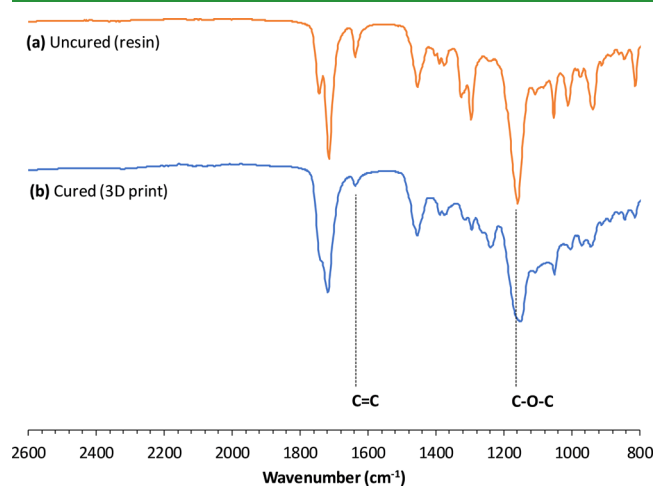


Figure 2. FTIR spectra for (a) uncured BMPR-10 and (b) cured BMPR-10 printed on a DLP 3D printer.

during 3D printing, as indicated by the significant decrease of the signal representing the C=C stretch vibration (1635 cm⁻¹) and the shift of the C–O–C oscillation (1165 to 1150 cm⁻¹).

Rook tower prototypes with a complex architecture were printed, and their visual evaluation demonstrates good print quality with smooth surface finishing (Figure 3a–c). The

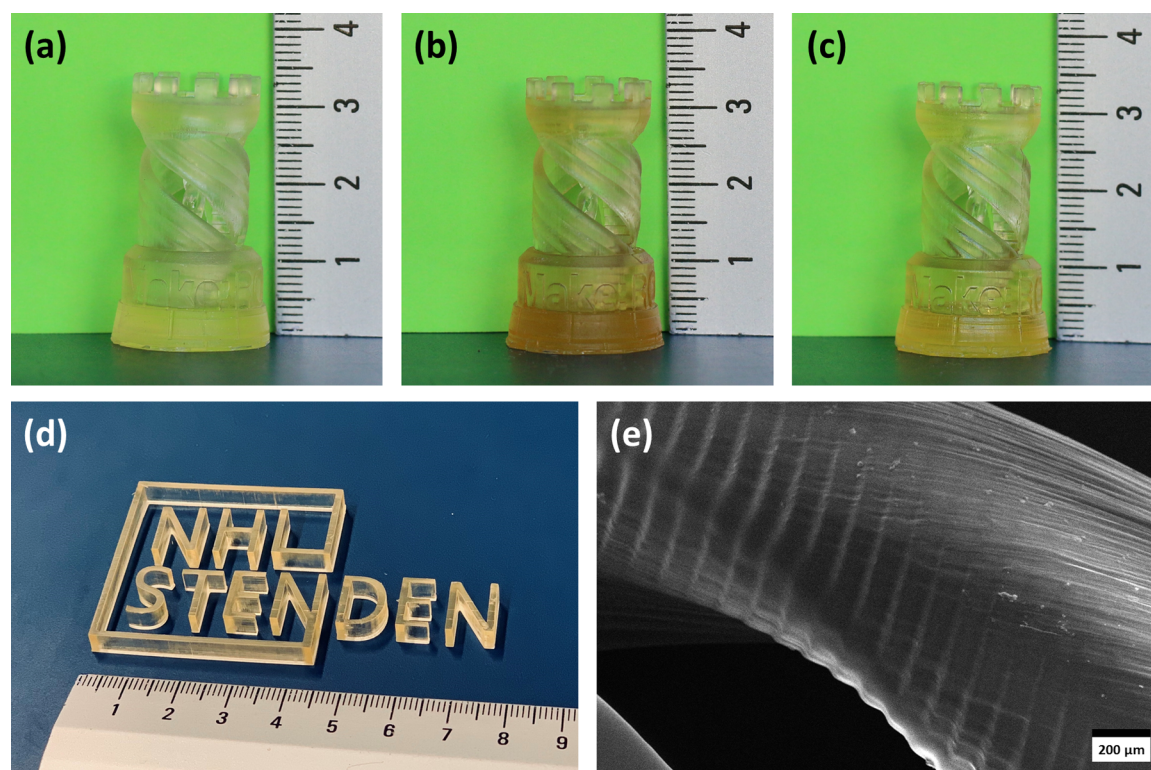


Figure 3. Pictures of the rook tower prototype printed with (a) BMPR-06, (b) BMPR-09, and (c) BMPR-10. (d) Picture of the university logo printed with BMPR-09. (e) SEM image of the internal double helix of the rook tower prototype printed with BMPR-09. All products were manufactured on a DLP 3D printer. The scale of the ruler is centimeters.

rook towers from BMPR-09 and BMPR-10 have a more intense color related to the amber-colored ESOMA. The university logo (Figure 3d) shows that high edge definition is achieved with the designed process. The SEM image (Figure 3e) of the internal double helix within the prototype reveals a complete fusion between the layers of 100 μm , which emphasizes the compatibility of our renewable resins with DLP technology up to the print-layer level. The vertical edges of the helices are slightly serrated, caused by the top surface of a layer receiving a larger UV dose in comparison to the back surface.³⁸

Product Performance. The glass transition temperature of the printed objects, derived from the peak maximum of the damping factor (Figure 4), is depicted in Table 3. Products from BMPR-09 exhibit the highest glass transition at 97 $^{\circ}\text{C}$. Subsequently, the cross-link density was calculated from the storage modulus in the rubbery region. BMPR-09 gives rise to a higher cross-link density than BMPR-10 (Table 3). This is related to the presence of ESOMA₃ within BMPR-09 with respect to ESOMA₂ in BMPR-10. A higher methacrylate functionality leads to a denser polymer network and hence a higher ν_e .³⁹

Figure 5 visualizes the tensile properties of the printed objects by showing the representative stress–strain curves. The repeatability of the 3D printing method was investigated by preparing, printing, and tensile testing two batches of identical composition for all bioresins. This results in the same trend in the tensile properties (Figure 5), and no significant difference in the E modulus was observed between the different batches of equal resin composition. Furthermore, the elastic moduli of the printed objects (Table 3), all tested normal to the print layers, were similar to those of the mold-

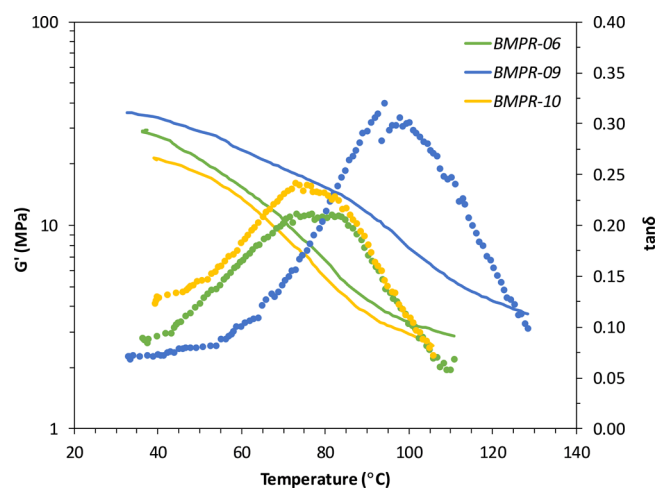


Figure 4. DMA curves for products from BMPR-06, BMPR-09, and BMPR-10, all printed on a DLP 3D printer. Solid lines represent G' data, dotted curves represent values for $\tan \delta$.

cured products (Table 2), demonstrating the competitiveness of the stereolithographic printing process with respect to traditional casting techniques.

The deformation energy, defined as the area under a stress–strain curve, is related to the toughness. While stiffness and tensile strength of thermosets typically increase for higher cross-link densities, toughness decreases.¹⁵ As a matter of fact, printed objects from BMPR-10 and BMPR-06 demonstrate a higher deformation energy in comparison to BMPR-09, while the cross-link density is lower (Table 3). In addition, BMPR-09 gives rise to the highest E modulus and

Table 3. Characteristics of 3D Printed Products from Biobased Resins

resins	T_g ($^{\circ}\text{C}$)	ν_e ($\text{mol}\cdot\text{m}^{-3}$)	E (MPa)	ϵ_B (%)	σ_M (MPa)	U_T ($\text{J}\cdot\text{m}^{-3}$)
BMPR-06	80.2	300	870 ± 44	18 ± 3	36.4 ± 0.4	510 ± 88
BMPR-09	96.9	377	1007 ± 30	10 ± 2	43.7 ± 0.3	323 ± 70
BMPR-10	78.1	257	727 ± 12	24 ± 3	28.3 ± 0.3	560 ± 82

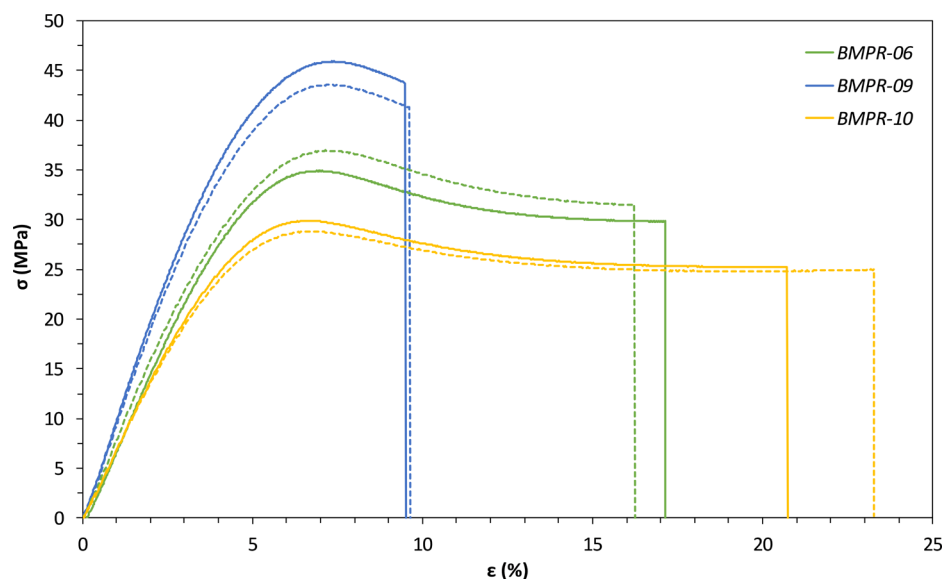


Figure 5. Representative stress–strain curves for products from BMPR-06, BMPR-09, and BMPR-10, all printed on a DLP 3D printer. Dashed lines correspond to the results from the second resin batch.

tensile strength with values of 1.0 GPa and 44 MPa, respectively.

While both photoresins have an equal monomer-to-oligomer ratio, BMPR-09 gives rise to a significantly higher elastic modulus than BMPR-06. In other words, the fully methacrylated system based on ESOMA₃ provides more stiffness. When comparing both methacrylate resins, BMPR-09 has a higher E modulus than BMPR-10, due to the higher cross-link density that results from the incorporation of methacrylate oligomer with higher functionality. Hence, the tensile properties can be tuned by changing the chemical composition (acrylate versus methacrylate) or the number of side groups in the oligomer.

In general, the formulated biobased resins based on soybean oil demonstrate good mechanical performance. The ultimate properties such as stiffness and glass transition temperature are superior to pure ESOA resins and comparable to recently reported values for alternative soybean oil-based epoxy acrylate resins cured by conventional methods.^{28,29} In addition, the tensile properties of BMPR-09 are significantly higher than those of the commercial clear photoresin of Autodesk (PR48), as depicted in Figure S6. The clear resin of Liqcreate, Deep Blue (LCDB), demonstrates the highest E modulus and tensile strength, while the biobased resins have a higher elongation at break. Both PR48 and LCDB show a lower toughness (20 and 294 $\text{J}\cdot\text{m}^{-3}$, respectively) in comparison to the bioresins (323–560 $\text{J}\cdot\text{m}^{-3}$). Hence, the mechanical performance of printed BMPRs is competitive with commercial counterparts.

CONCLUSION

In this study, we have developed photocurable resins based on renewable methacrylate oligomers for 3D printing.

Epoxidized soybean oil was methacrylated, leading to products with a functionality of 2.3 and 3.0. A library of photoresins was generated by mixing soybean oil (meth)acrylates with monofunctional diluents and a photoinitiator in various compositions. Resins with biorenewable carbon contents of 77 to 80% and viscosities of 0.5 to 1.5 Pa·s were selected for stereolithographic 3D printing. The manufactured prototypes demonstrate the compatibility of the biobased resins with DLP technology up to the microscopic level. The fully methacrylated resin based on soybean oil methacrylate enhances the stiffness and tensile strength with respect to the soybean oil acrylate. By lowering the methacrylate functionality, the elastic modulus decreases as a result of the lower cross-link density while toughness increases. The biobased resins provide both a sustainable and competitive alternative to facilitate the increasing demand for materials in additive manufacturing.

ASSOCIATED CONTENT

Supporting Information

The Supporting Information is available free of charge at <https://pubs.acs.org/doi/10.1021/acsapm.9b01143>.

Additional working curves, object design, ¹H NMR spectra, stress-strain curves, and rheological data are included (PDF)

AUTHOR INFORMATION

Corresponding Author

Vincent S.D. Voet – Professorship Sustainable Polymers, NHL Stenden University of Applied Sciences, 7811 Emmen, The Netherlands; orcid.org/0000-0003-0863-0616; Email: vincent.voet@nhlstenden.com

Authors

Jarno Guit – Professorship Sustainable Polymers, NHL Stenden University of Applied Sciences, 7811 Emmen, The Netherlands

Marjory B.L. Tavares – Professorship Sustainable Polymers, NHL Stenden University of Applied Sciences, 7811 Emmen, The Netherlands

Jerzy Hul – Liqcreate, 3442 Woerden, The Netherlands

Chongnan Ye – Professorship Sustainable Polymers, NHL Stenden University of Applied Sciences, 7811 Emmen, The Netherlands; Macromolecular Chemistry and New Polymeric Materials, Zernike Institute for Advanced Materials, University of Groningen, 9747 Groningen, The Netherlands

Katja Loos – Macromolecular Chemistry and New Polymeric Materials, Zernike Institute for Advanced Materials, University of Groningen, 9747 Groningen, The Netherlands;

orcid.org/0000-0002-4613-1159

Jan Jager – Professorship Sustainable Polymers, NHL Stenden University of Applied Sciences, 7811 Emmen, The Netherlands

Rudy Folkersma – Professorship Sustainable Polymers, NHL Stenden University of Applied Sciences, 7811 Emmen, The Netherlands

Complete contact information is available at:
<https://pubs.acs.org/10.1021/acsapm.9b01143>

Author Contributions

The manuscript was written through contributions of all authors. All authors have given approval to the final version of the manuscript.

Funding

This work was supported by the province of Drenthe, the municipality of Emmen, and the Green Polymer Application Centre (Green PAC) as part of Project 313005, “3D Printing in Production”.

Notes

The authors declare no competing financial interest.

ACKNOWLEDGMENTS

Jur van Dijken is kindly acknowledged for his support on the thermal and mechanical analysis. The authors thank Xiaotian Zhu for assistance with SEM imaging.

REFERENCES

- (1) Berman, B. 3-D printing: The new industrial revolution. *Bus. Horizons* **2012**, *55*, 155–162.
- (2) Weller, C.; Kleer, R.; Piller, F. T. Economic implications of 3D printing: Market structure models in light of additive manufacturing revisited. *Int. J. Prod. Econ.* **2015**, *164*, 43–56.
- (3) Core, B. *3D Printing Materials 2019–2029: Technology and Market Analysis*; IDTechEx: Cambridge, U.K., 2019.
- (4) Ligon, S. C.; Liska, R.; Stampfl, J.; Gurr, M.; Mühlhaupt, R. Polymers for 3D Printing and Customized Additive Manufacturing. *Chem. Rev.* **2017**, *117*, 10212–10290.
- (5) Van Wijk, A.; van Wijk, I. *3D Printing with Biomaterials: Towards a Sustainable and Circular Economy*; IOS Press: Amsterdam, The Netherlands, 2015.
- (6) Adharies, A.; Petrovic, D. M.; Özdamar, I.; Woortman, A. J. J.; Loos, K. Environmentally friendly pathways towards the synthesis of vinyl-based oligocelluloses. *Carbohydr. Polym.* **2018**, *193*, 196–204.
- (7) Gross, B. C.; Erkal, J. L.; Lockwood, S. Y.; Chen, C.; Spence, D. M. Evaluation of 3D printing and its potential impact on biotechnology and the chemical sciences. *Anal. Chem.* **2014**, *86*, 3240–3253.
- (8) Hull, C. W. Apparatus for production of three-dimensional objects by stereolithography. U.S. Patent 4575330. 1986.

(9) Chia, H. N.; Wu, B. M. Recent advances in 3D printing of biomaterials. *J. Biol. Eng.* **2015**, *9*, 4.

(10) Stampfl, J.; Baudis, S.; Heller, C.; Liska, R.; Neumeister, A.; Kling, R.; Ostendorf, A.; Spitzbart, M. Photopolymers with tunable mechanical properties processed by laser-based high-resolution stereolithography. *J. Micromech. Microeng.* **2008**, *18*, 125014.

(11) Van Noort, R. The future of dental devices is digital. *Dent. Mater.* **2012**, *28*, 3–12.

(12) Bhatia, S. K.; Ramadurai, K. W. *3D Printing and Bio-Based Materials in Global Health*; Springer: Cham, Switzerland, 2017.

(13) Wu, G. H.; Hsu, S. H. Review: Polymeric-Based 3D Printing for Tissue Engineering. *J. Med. Biol. Eng.* **2015**, *35*, 285–292.

(14) Skoog, S. A.; Goering, P. L.; Narayan, R. J. Stereolithography in tissue engineering. *J. Mater. Sci.: Mater. Med.* **2014**, *25*, 845–856.

(15) Ligon, S. C.; Schwentenwein, M.; Gorsche, C.; Stampfl, J.; Liska, R. Toughening of photo-curable polymer networks: a review. *Polym. Chem.* **2016**, *7*, 257–286.

(16) Elliott, J.; Bowman, C. Predicting network formation of free radical polymerization of multifunctional monomers. *Polym. React. Eng.* **2002**, *10*, 1–19.

(17) Chattopadhyay, D. K.; Panda, S. S.; Raju, K. V. Thermal and mechanical properties of epoxy acrylate/methacrylates UV cured coatings. *Prog. Org. Coat.* **2005**, *54*, 10–19.

(18) Kannurpatti, A. R.; Anseth, J. W.; Bowman, C. N. A study of the evolution of mechanical properties and structural heterogeneity of polymer networks formed by photopolymerizations of multifunctional (meth)acrylates. *Polymer* **1998**, *39*, 2507–2513.

(19) Yang, E.; Miao, S.; Zhong, J.; Zhang, Z.; Mills, D. K.; Zhang, L. G. Bio-Based Polymers for 3D Printing of Bioscaffolds. *Polym. Rev.* **2018**, *58*, 668–687.

(20) Melchels, F. P.W.; Feijen, J.; Grijpma, D. W. A review on stereolithography and its applications in biomedical engineering. *Biomaterials* **2010**, *31*, 6121–6130.

(21) Melchels, F. P.W.; Feijen, J.; Grijpma, D. W. A Poly(D,L-Lactide) Resin For The Preparation Of Tissue Engineering Scaffolds By Stereolithography. *Biomaterials* **2009**, *30*, 3801–3809.

(22) Lim, L. T.; Auras, R.; Rubino, M. Processing technologies for poly(lactic acid). *Prog. Polym. Sci.* **2008**, *33*, 820–852.

(23) Gonçalves, F. A. M. M.; Costa, C. S. M. F.; Fabela, I. G. P.; Farinha, D.; Faneca, H.; Simões, P. N.; Serra, A. C.; Bártolo, P. J.; Coelho, J. F. J. 3D printing of new biobased unsaturated polyesters by microstereo-thermal-lithography. *Biofabrication* **2014**, *6*, No. 035024.

(24) Sutton, J. T.; Rajan, K.; Harper, D. P.; Chmely, S. C. Lignin-Containing Photoactive Resins for 3D Printing by Stereolithography. *ACS Appl. Mater. Interfaces* **2018**, *10*, 36456–36463.

(25) Skliutas, E.; Kasetaitė, S.; Jonusauskas, L.; Ostrauskaite, J.; Malinauskas, M. Photosensitive naturally derived resins toward optical 3-D printing. *Opt. Eng.* **2018**, *57*, No. 1.

(26) Lebedevaite, M.; Ostrauskaite, J.; Skliutas, E.; Malinauskas, M. Photoinitiator free resins composed of plant-derived monomers for the optical m-3D printing of thermosets. *Polymers* **2019**, *11*, 116.

(27) Behera, D.; Banthia, A. K. Synthesis, characterization, and kinetics study of thermal decomposition of epoxidized soybean oil acrylate. *J. Appl. Polym. Sci.* **2008**, *109*, 2583–2590.

(28) Wu, Q.; Hu, Y.; Tang, J. J.; Zhang, J.; Wang, C. N.; Shang, Q. Q.; Feng, G. D.; Liu, C. G.; Zhou, Y. H.; Lei, W. High-performance Soybean Oil-based Epoxy Acrylate Resins: “Green” Synthesis and Application in UV-Curable Coatings. *ACS Sustainable Chem. Eng.* **2018**, *6*, 8340–8349.

(29) Liu, C. G.; Dai, Y.; Hu, Y.; Shang, Q. Q.; Feng, G. D.; Zhou, J.; Zhou, Y. H. Highly Functional Unsaturated Ester Macromonomer Derived from Soybean Oil: Synthesis and Copolymerization with Styrene. *ACS Sustainable Chem. Eng.* **2016**, *4*, 4208–4216.

(30) Miao, S.; Zhu, W.; Castro, N. J.; Nowicki, M.; Zhou, X.; Cui, H.; Fisher, J. P.; Zhang, L. G. 4D printing smart biomedical scaffolds with novel soybean oil epoxidized acrylate. *Sci. Rep.* **2016**, *6*, 27226.

(31) Voet, V. S. D.; Strating, T.; Schnelting, G. H. M.; Dijkstra, P.; Tietema, M.; Xu, J.; Woortman, A. J. J.; Loos, K.; Jager, J.

Folkersma, R. Biobased Acrylate Photocurable Resin Formulation for Stereolithography 3D Printing. *ACS Omega* **2018**, *3*, 1403–1408.

(32) Voet, V. S. D.; Schnelting, G. H. M.; Xu, J.; Loos, K.; Folkersma, R.; Jager, J. Stereolithographic 3D Printing with Renewable Acrylates. *J. Visualized Exp.* **2018**, No. 139, No. e58177.

(33) Thingiverse – Digital Designs for Physical objects. <https://www.thingiverse.com>. (accessed June 2019).

(34) Li, Y.; Sun, X. S. Synthesis and characterization of acrylic polyols and polymers from soybean oils for pressure-sensitive adhesives. *RSC Adv.* **2015**, *5*, 44009–44017.

(35) Weng, Z.; Zhou, Y.; Lin, W.; Senthil, T.; Wu, L. Structure-property relationship of nano enhanced stereolithography resin for desktop SLA 3D printer. *Composites, Part A* **2016**, *88*, 234–242.

(36) Scalera, F.; Esposito Corcione, C.; Montagna, F.; Sannino, A.; Maffezzoli, A. Development and Characterization of UV Curable Epoxy/Hydroxyapatite Suspensions for Stereolithography Applied to Bone Tissue Engineering. *Ceram. Int.* **2014**, *40*, 15455–15462.

(37) Steyrer, B.; Busetti, B.; Harakaly, G.; Liska, R.; Stampfl, J. Hot Lithography vs. room temperature DLP 3D-printing of a dimethacrylate. *Additive Manufacturing* **2018**, *21*, 209–214.

(38) Gong, H.; Beauchamp, M.; Perry, S.; Woolley, A. T.; Nordin, G. P. Optical approach to resin formulation for 3D printed microfluidics. *RSC Adv.* **2015**, *5*, 106621–106632.

(39) Lu, J.; Khot, S.; Wool, R. P. New Sheet Molding Compounds Resins from Soybean Oil. I. Synthesis and Characterization. *Polymer* **2005**, *46*, 71–80.